

Si detectors for high energy particles

Contents

<p>1. <u>Characteristics</u> p.02</p> <p>2. <u>Si detectors for scintillator coupling</u> p.03</p> <p>3. <u>Si direct detectors</u> p.03</p>	<p>4. <u>New approaches</u> p.07</p> <p>5. <u>Applications</u> p.07</p>
---	---

Si detectors for high energy particles utilize one of two detection methods. One is the scintillator coupling type that indirectly detects high energy particles by converting them into scintillation light, while the other method detects the high energy particles directly. Si detectors used by these two methods include large-area Si PIN photodiodes, Si APD (avalanche photodiodes), large-area PSD (position sensitive detectors), and SSD (Si strip detectors).

The large-area Si PIN photodiodes for scintillator coupling have a photosensitive area up to 28 × 28 mm made from a single-crystal silicon wafer with high resistivity. Since these photodiodes are used in combination with a scintillator, their spectral response matches the scintillator emission wavelength. Even with the large photosensitive area, they deliver high-speed response.

The large-area Si PIN photodiodes for the direct detection method have a photosensitive area up to 48 × 48 mm. Since these photodiodes normally have a thin dead layer and a thick depletion layer, they offer high detection efficiency and can be used as ΔE detectors or E detectors.

The Si APD is a high-sensitivity detector capable of high-speed detection of weak light emitted from a scintillator. The large-area PSD is a non-segmented position detector and can also be used as a ΔE detector or an E detector as well as a detector of incident charged particle positions.

The SSD is a high-precision Si detector merging photodiode and IC technologies. A number of photosensitive areas (PN junctions) are fabricated on the substrate, in the form of strips in widths from a few microns to several dozen microns, so the incident position of high energy particles can be detected in micron units. This performance is widely utilized in high energy physics experiments as an elementary particle tracking detector (Si vertex detector).

Hamamatsu Si detectors for high energy particles have the following features.

- ❑ Low dark current, low noise
- ❑ ΔE detector: excellent thickness uniformity
- ❑ High radiation resistance
- ❑ High voltage tolerance
- ❑ Spectral response matching the scintillator emission wavelength

❖ Hamamatsu Si detectors for high energy particles

Type	Detection method	Features
Large-area Si PIN photodiode	Scintillator coupling	High-speed response even with large photosensitive area by applying a high reverse voltage Used in combination with scintillator (a type with scintillator and a type that user bond the scintillator are available) Photosensitive area: 28 × 28 mm max.
	Direct detection	Usable as ΔE detector and E detector For detecting energy of high energy particles Photosensitive area: 48 × 48 mm max.
Si APD	Scintillator coupling	High-speed, high-sensitivity photodiode having internal multiplication function Capable of measuring weak signals Mainly used in combination with scintillator
Large-area PSD	Direct detection	Usable as ΔE detector and E detector For detecting energy and two-dimensional incident position of high energy particles
SSD	Direct detection	For track detection of high energy particles Photodiode strip array achieves high position resolution with low noise.

1. Characteristics

1 - 1 Active area

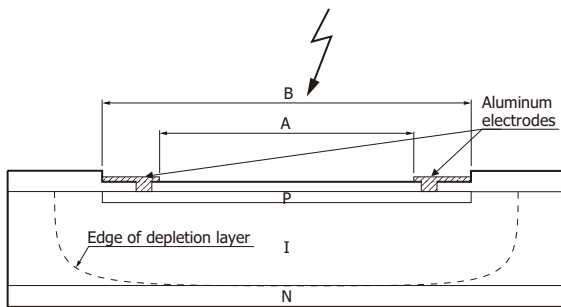
Light cannot pass through aluminum electrodes, but high energy particles pass through them easily. The active area of Si direct detectors is therefore defined as the P-layer region including the aluminum electrodes, while the active area of Si detectors for scintillator coupling is defined as the P-layer region excluding the aluminum electrodes [Figure 1-1].

If light strikes the periphery (not light-shielded) of a PN junction on a Si detector with scintillator, the carriers generated there are output as a signal. Likewise, radiation entering outside the active area of a Si direct detector generates a signal.

The insulation film, aluminum electrodes, and P-layer of the Si detector surface serve as dead layers causing energy loss, but the energy lost does not result in signal generation.

When a reverse voltage is applied to the Si detector, the depletion layer extends horizontally to some extent as well as along the detector thickness. If the active area must be accurately specified, then a P-layer as a guard ring is sometimes formed around the active area in order to absorb the excess carriers generated outside the guard ring.

[Figure 1-1] Cross section of Si detector



Active area
A: Si detector for scintillator coupling
B: Si direct detector

KSPDC0002EB

1 - 2 Dark current and junction capacitance

When a reverse voltage is applied to a Si detector, a small amount of current flows even in a dark state. This current, called the dark current or leakage current, becomes larger as the reverse voltage is increased and is a major cause of noise. Dark current consists of two components: a thermally generated current and a current generated from defects in the silicon crystal and from the interface of the silicon oxide film. These currents flow in a reverse direction of the diode.

The junction capacitance of a Si detector is determined by the area of the P-layer and the thickness of the depletion layer, and can be approximated by equation (1-1).

$$C = \frac{\epsilon_0 \epsilon_s S}{W} \dots\dots\dots (1-1)$$

C : junction capacitance
 ϵ_0 : permittivity in vacuum
 ϵ_s : specific permittivity of silicon
S : area of P-layer
W : thickness of depletion layer

The junction capacitance is minimized when the I-layer is fully depleted.

The recommended reverse voltage for each Si detector is the voltage required for full depletion of the substrate. Operating a Si detector at its recommended voltage not only minimizes the junction capacitance but also lowers the series resistance as the I-layer is fully depleted. Lowering the junction capacitance and series resistance will also improve the response speed and reduce noise.

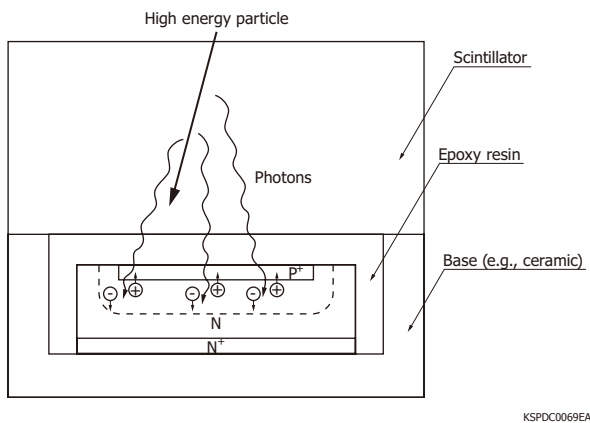
1 - 3 Response speed

There are two major factors that determine the response speed of Si detectors. One factor is the time constant determined by the terminal capacitance, series resistance of the Si detector, and the externally connected load resistance. The other factor is the time required for the signal charge generated in the silicon to reach the electrode (carrier collection time). This carrier collection time is also categorized as the time during which the carriers flow as a diffusion current outside the depletion layer and the time (drift time) during which carriers flow in the depletion layer due to the electric field. When fully depleted by reverse voltage, the drift time determines the carrier collection time. If the time constant of the Si detector is small, then the response speed is limited by the carrier collection time. On the other hand, in large-area Si detectors, the response speed is limited by a time constant.

2. Si detectors for scintillator coupling

Si detectors for scintillator coupling indirectly detect high energy particles by detecting light emitted from a scintillator. The structure of these detectors is shown in Figure 2-1. Scintillators can usually be made large and thick, so they are effective in detecting particles where Si direct detectors would not be able to detect all the energy because particles would penetrate through. Si detectors for scintillator coupling are widely used to detect charged particles and gamma-rays. Since these Si detectors are optically coupled to a scintillator, they use Si PIN photodiodes and the like that have a high quantum efficiency at the scintillator emission wavelength. These Si PIN photodiodes should have a large photosensitive area for optical coupling to a scintillator. The operating principle of the Si detectors for scintillator coupling is the same as that of general photodiodes (see “X-ray detectors technical note | 1. Si photodiodes”).

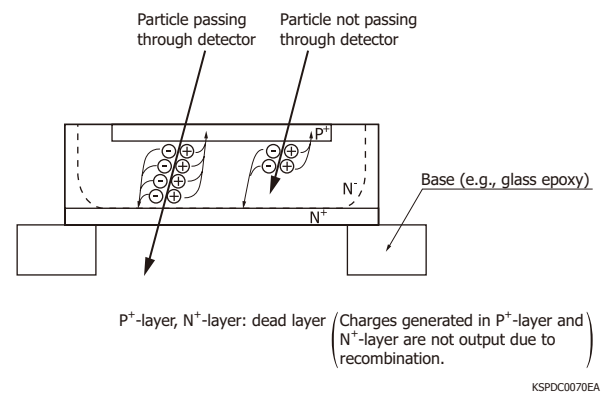
[Figure 2-1] Structure of Si detector for scintillator coupling



3. Si direct detectors

Si direct detectors including large-area Si PIN photodiodes, PSD, and SSD detect charges internally ionized by radiation energy that directly enters the Si detector. Si direct detectors offer high energy resolution, high-speed response, and low noise. Figure 3-1 shows the structure of Si direct photodiodes. Si direct detectors are not covered with a protective film such as resin. This is intended to suppress the energy loss that occurs in the dead layer on the Si detector surface where the charge particles enter.

[Figure 3-1] Structure of direct photodiode



When charged particles such as alpha-rays and heavy ions strike a Si detector, their energy dissipates along a linear track whose length is determined by the type and energy of the incident charged particles, and electron-hole pairs are generated by means of the Coulomb interaction of a charged particle with electrons. The number of the generated electron-hole pairs does not depend on the type of charged particle but rather on the energy loss (at 300 K, one electron-hole pair is generated on average per each 3.62 eV). The energy loss can therefore be estimated by detecting the amount of this charge.

The E detector is a thick detector, so it does not allow the charged particles to pass through, thereby capturing the total energy (E). To achieve this, the E detector must have a depletion layer thick enough to cover the whole track (range) from the incident point to the stop point of the charged particles.

The ΔE detector is a transmission type detector that captures the energy that a charged particle loses as it passes through the detector. When two or more ΔE detectors are stacked on each other, the incident angle of the charged particle can be detected by finding the position where the charged particle passes through each ΔE detector.

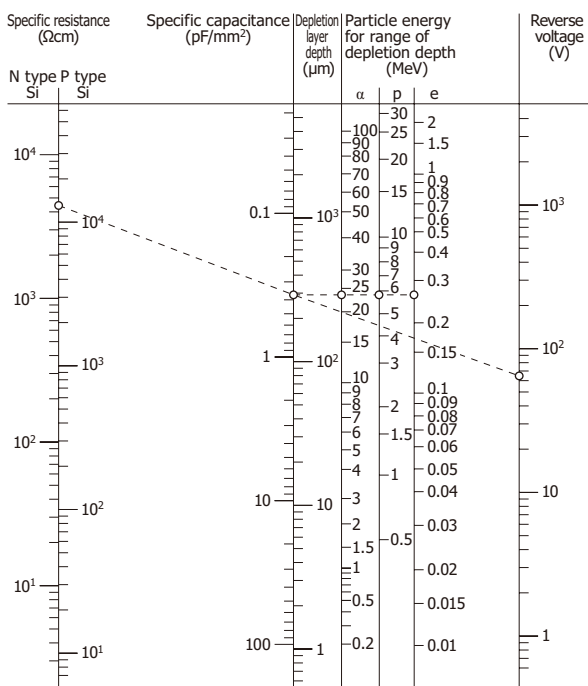
One way of identifying particles is to combine the ΔE detector, which is a transmission type detector, with a thick E detector [Fig. 5-8]. The ΔE detector can detect

specific energy loss (dE/dx) of transmitted particles, and it can estimate total energy (E) of the particles along with the energy detected by the E detector. Each particle has a unique value of $(dE/dx) \times E$, making it possible to identify the type of incident particle. Using multiple ΔE detectors capable of detecting position, it is possible to detect incident angle and incident position, in addition to energy of incident particles.

Beta-rays differ from alpha-rays and heavy ions in that their track is nonlinear and the range is long because their mass is relatively small and energy loss occurs in the process of emitting electromagnetic waves.

Figure 3-2 shows the relationship between the energy of typical charged particles (α : alpha-rays, p: protons, e: electrons), the resistivity of the silicon wafer, the capacitance value (specific capacitance) per unit area, the depletion layer thickness (depth) required to detect the charged particle, and the reverse voltage (bias voltage) applied to extend the depletion layer. Use this nomograph as a guide to select the Si detector that matches the application.

[Figure 3-2] Si detector parameter nomograph



1 μm Si=0.2325 mg/cm^2
1 mg/cm^2 Si=4.3 μm

Nomograph showing mutual relation between Si detector parameters (similar to nomograph originally reported by J. L. Blankenship)

KSPDC004EC

■ References

IEEE transactions on nuclear science, Vol. NS-7, 190-195 (1960)

3 - 1 Thickness of depletion layer

The E detector must have a depletion layer whose thickness is more than the range of the charged particles

to be detected. The following points must be considered when setting the depletion layer thickness.

- Increasing the reverse voltage extends the depletion layer and lowers the terminal capacitance and series resistance which are major causes of noise.
- Increasing the electric field on the depletion layer improves the response speed but increases the dark current, resulting in larger noise.

When the depletion layer is partially extended relative to the Si detector substrate thickness, this state is called “partial depletion.” On the other hand, a state where the depletion layer is fully widened and cannot be extended any further even by increasing the reverse voltage is called “full depletion.” The ΔE detector is used under the full depletion condition.

3 - 2 Channeling effect

The channeling effect is a phenomenon in which charged particles moving along the crystal lattice lose less energy and therefore reach deeper. If this channeling effect occurs, charged particles that should normally stop inside the depletion layer might instead reach the outside of the depletion layer or might pass entirely through the detector. Therefore, in charged particle track detection, attention must be given to the channeling effect.

3 - 3 Pulse height variations

In actual Si detector operation, the generated electron-hole pairs are not completely detected, and this causes pulse height variations. Even if charged particles with the same energy enter the detector, their outputs are not always the same. This phenomenon occurs from the following three factors.

The first factor is thin dead layers on the front and rear sides of the Si detector, which do not become depleted. In E detectors, dead layers made up of a protective film and diffusion layer section on the front surface can cause pulse height variations. In ΔE detectors, the dead layer caused by the rear side diffusion layer can also cause pulse height variations.

The second factor is the crystal defects formed in the depletion layer. Radiation entering the Si detector forms crystal defects in the depletion layer, causing an increase in dark current. The dark current increases almost in proportion to the amount of absorbed radiation, and gradually degrades Si detector performance. Because the crystal defects that form in the depletion layer serve as recombination centers, some of the electron-hole pairs recombine there and are not output.

The third factor is the recombination of electron-hole

pairs that occurs due to high-density plasma created along the particle track.

Effects caused by the second and third factors can be reduced by increasing the electric field strength in the depletion layer since this lowers the probability that electron-hole pairs will recombine.

3 - 4 Noise and energy resolution

The most important point to consider in measuring the energy resolution is statistical noise. Since statistical noise exists as a fundamental factor, the total number of electron-hole pairs generated is not consistent even when particles with the same energy enter the detector. This statistical noise cannot be ignored when measuring the energy resolution. Assuming that incident particles will generate “N” pairs of electrons and holes on the average, the energy resolution [R(FWHM)] determined by the statistical noise is expressed in equation (3-1).

$$R = 2.35 \sqrt{F/N} \dots\dots\dots (3-1)$$

Here, F is a coefficient called the Fano factor. Reports of many experimental results using Si detectors indicate that this F value is approx. 0.1.

Another factor that affects energy resolution is random noise generated throughout the entire system including the Si detector and its circuit. This random noise increases as the dark current and junction capacitance of the Si detector become larger.

During ΔE detection of charged particles such as alpha-rays and protons, there is a basic fluctuation (2 to 3% on average) in the particle range. The number of electron-hole pairs generated relative to the same thickness is therefore not constant. There is also inconsistencies in the detector thickness. These factors adversely affect the energy resolution.

3 - 5 Si detectors for position detection

The following sections describe large-area two-dimensional PSD and SSD that are Si direct detectors capable of position detection.

» Large-area two-dimensional PSDs

The large-area two-dimensional PSD has a uniform, highly resistive P-layer or N-layer on which four electrodes are formed. A charge produced by the input of a high energy particle is collected by the four electrodes through the highly resistive layer. The energy loss of the particle can be detected from the total amount of the charge. The position of the incident particle can also be detected because the ratio of the

charge collected by each electrode correlates with the position where the charge was produced.^{2) 6)}

The PSD offers the advantages of a simple structure and a capability of position detection on its large photosensitive area. However, if two or more particles simultaneously enter a PSD (multi-hit), then detecting the particle positions is impossible. Furthermore, since the electrodes are connected to each other through the resistive layer, the thermal noise becomes higher than in photodiodes. The PSD is for this reason usually used to detect heavy ions whose specific energy loss is large among charged particles.

» SSD

The SSD has a photodiode array structure of strips in widths of several dozen microns. The photosensitive area consists of a large number of strips (channels), so when a particle enters the SSD, signal outputs are distributed to one or multiple strips corresponding to the position of the incident particle. The position of the incident particle can be obtained at a resolution smaller than the strip pitch. The SSD has low noise and detects positions even if multiple particles enter simultaneously (multi-hit detection). Hamamatsu SSDs have the following features:

- Low voltage operation due to using high-resistivity silicon substrate
- Stable operation maintained due to low dark current and high voltage tolerance
- Low defect channel ratio (less than 1%)
- AC readout type provides high radiation resistance by using poly-silicon biasing.

⚙ Readout method

SSD is classified into DC readout type or AC readout type. In the DC readout type, each strip diffusion layer is DC-coupled to an aluminum electrode. In the AC readout type, however, each strip diffusion layer is AC-coupled to an aluminum electrode. Compared to the DC readout type SSD, the AC readout type SSD has the advantage of good compatibility with the readout IC chip since the dark current (DC current) from each strip does not flow into the signal line. In the AC readout type SSD, a reverse voltage must be applied to each strip from the bias line. This reverse voltage is applied by the “punch-through” method or the “poly-silicon” method. Hamamatsu SSDs use the poly-silicon method as standard because of its superior radiation hardness.^{3) 9)}

[Figure 3-3] DC readout type

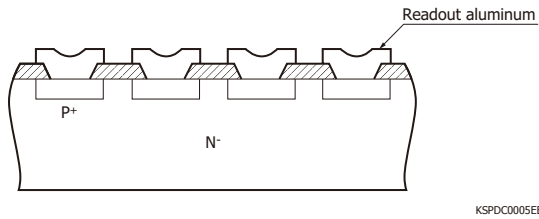
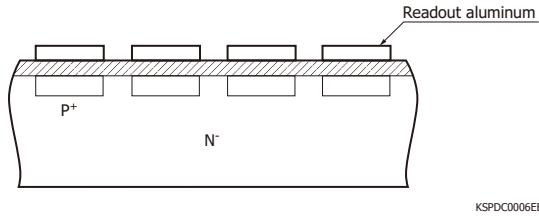


[Figure 3-4] AC readout type



⚙ Single-sided SSD and double-sided SSD

Single-sided SSDs (SSSDs) have strip structures only on one side and perform one-dimensional position detection. Double-sided SSDs (DSSDs) have strip structures on both sides and allow two-dimensional position detection with a single piece of SSD.⁵⁾

[Figure 3-7] Single-sided SSD

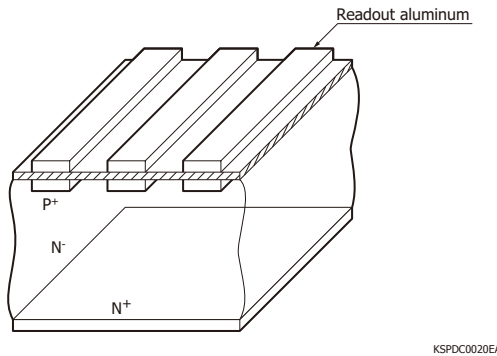
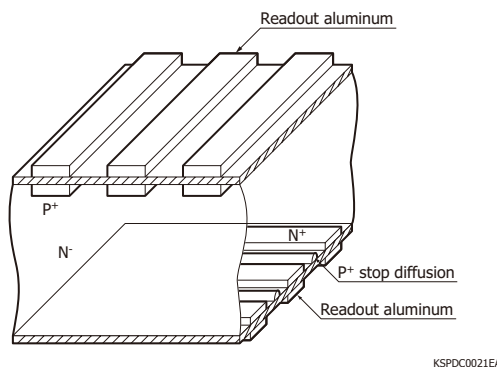


[Figure 3-8] Double-sided SSD



⚙ Ladder module assembly using single-sided SSDs

Although the SSD is sometimes used as a single piece, multiple SSDs are normally used while arrayed or stacked. For example, when using SSDs as particle tracking detectors in elementary particle experiments, multiple SSDs are joined in a ladder configuration and

a readout circuit is attached to the end piece to form a so-called ladder module. A large active area can then be obtained by placing these modules in a concentric circle at the point where particle collision (annihilation) takes place. The particle track can then be measured by processing data captured by these SSDs.

When assembling ladder modules capable of detecting a two-dimensional position by bonding two SSDs back-to-back, the readout electrode pads from both sides must be placed on the same edge. In this case, one method (double metal layer readout type) places the readout electrodes in a direction different from the strips, using either side having a double metal layer (DML) structure. In another method (nonorthogonal readout type) the strip angle on one side is tilted slightly to the other side. The structure of the nonorthogonal readout type has poorer position resolution on either side. However, this structure is simpler since no DML is used.

4. New approaches

In high energy physics experiments, there is a growing demand for larger size detectors due to the larger amounts of energy that must be detected. Hamamatsu is developing large-area Si detectors. In order to tile multiple Si detectors, we are also developing photodiodes compatible with flip-chip bonding and fully depleted photodiodes having small dead space.

We have already developed thin type ΔE detectors (10 μm thick or more) with superior thickness uniformity and are also developing thin dead layer type detectors. In the next particle collision experiments such as the HL-LHC (High Luminosity - Large Hadron Collider) scheduled to start from 2020 or later, the track detectors will be placed in such harsh environments as to be subject to a five to ten times greater radiation intensity than in the LHC project (experiments started in 2008). Hamamatsu is currently developing a high radiation tolerant SSD that can be used under these environments.

Si APD and MPPC are detectors capable of detecting very weak scintillation light. Because of their advantages of being compact, highly stable, and unaffected by magnetic fields, these detectors are likely useful not only in calorimeter detectors in high energy physics experiments but also in new fields such as medicine and bioscience.

5. Applications

5-1 Particle collision experiments

SSDs has been used as position detectors for high energy particles in many particle collision experiments (DELPHI, KEK-B, CDF, CLEO, ZEUS, etc.).
4) 10) 11) 12) 13)

Multiple SSD layers are arranged near the particle collision point in order to detect the tracks of elementary particles generated by the collision.

The Belle experimental apparatus [Figure 5-1] using electron-positron collider at the High Energy Accelerator Research Organization (KEK), uses our double-sided SSDs [Figure 5-2] and had verified in 2001 the CP symmetry violation of B meson predicted by the Kobayashi - Maskawa theory.²⁰⁾ Makoto Kobayashi and Toshihide Maskawa won the Nobel Prize in Physics in 2008.

In the LHC project by the European Organization for Nuclear Research (CERN) in Switzerland, an accelerator ring approx. 27 km in circumference is accelerating protons up to seven trillion electron volts in order to produce proton-proton collisions. The elementary particles resulting from these collisions are then detected. The major objective of this experiment was to verify the existence of the Higgs boson which was the only particle that was not yet observed (considered a particle that gives mass to matter). Its existence was verified in 2013. Peter Higgs and François Englert who predicted the existence of Higgs boson half a century ago were awarded the Nobel Prize in Physics in 2013.

The ATLAS experimental apparatus [Figure 5-3] in the LHC project uses approx. 14000 Hamamatsu SSDs as particle track detectors,¹⁴⁾ and the CMS experimental apparatus [Figure 5-4] uses approx. 22000 SSDs^{15) 16)} as particle track detectors. Our SSDs are also used in the ALICE and LHC-b experiments to detect particle tracks with accuracy down to a few dozen microns.

The electromagnetic calorimeter in the CMS experimental apparatus also uses 140000 Hamamatsu APDs as photo detectors for lead-tungstate scintillators.

[Figure 5-1] Belle experimental apparatus

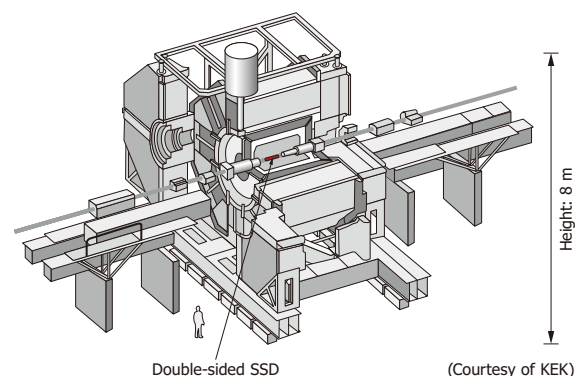


[Figure 5-2] Double-sided SSD modules used in the Belle experiment

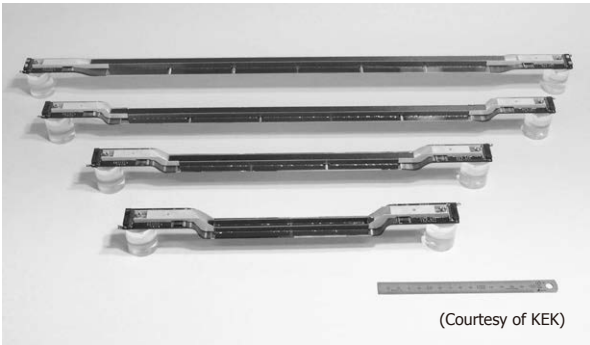


[Figure 5-3] ATLAS experimental apparatus

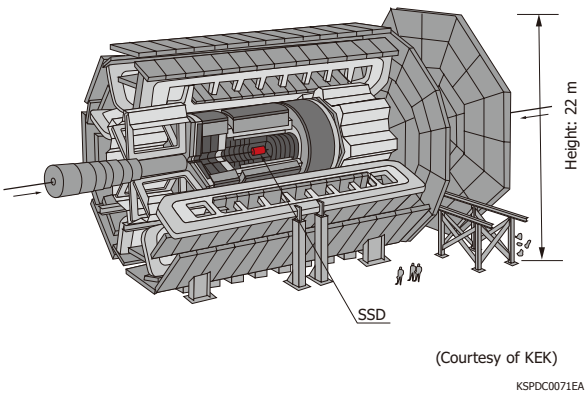
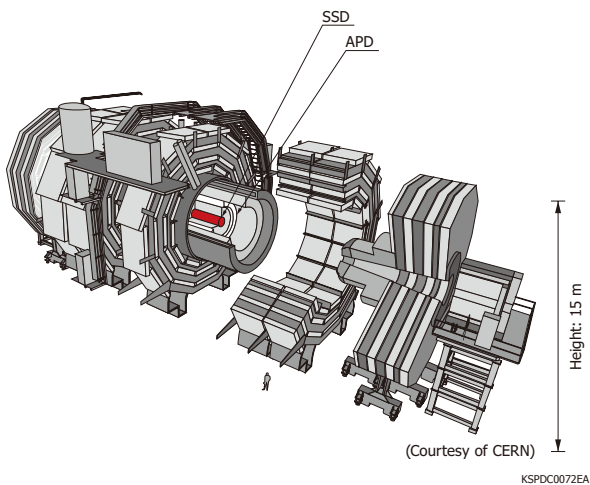


[Figure 5-4] CMS experimental apparatus



5 - 2 FGST (Fermi Gamma-ray Space Telescope) detectors*

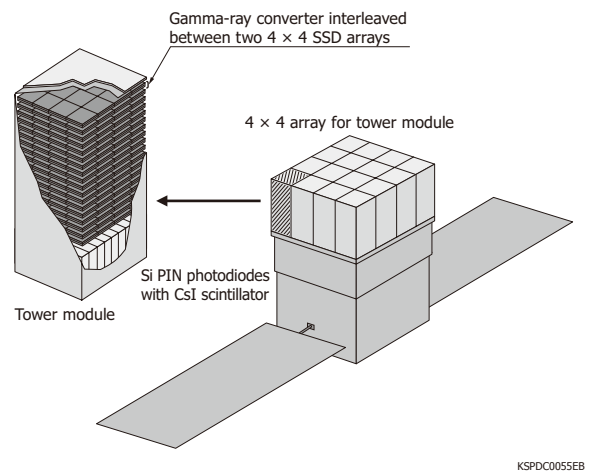
The NASA's FGST (satellite launched and experiment started in 2008) is a project for observing the universe in the gamma-ray region. The objectives of this project included understanding many mysteries in the universe such as gamma-ray bursts that release a huge amount of energy equal to that from the entire life of a sun in a short time ranging from only several seconds to several hundred seconds. Other phenomena to observe included the formation of colossal jets

extending to several dozen light-years in the active galaxy nuclei and mechanisms that release gamma-rays at ultra-high energy of several billion to one trillion electron volts from active galaxy nuclei and the like.

Figure 5-5 shows the tower module (tower detector) used in the FGST detector. A gamma-ray converter (converting gamma-rays into electron-positron pairs) is inserted between two 4×4 SSD arrays. This set is stacked in more than a dozen layers to build the tower module. A total of approx. 9000 SSDs are used in the tower module and play an important role in detecting the directions from which gamma-rays arrive. Our Si PIN photodiodes are used in the calorimeter.^{17) 19)}

* Former name: GLAST detector

[Figure 5-5] Tower module used in the FGST detector

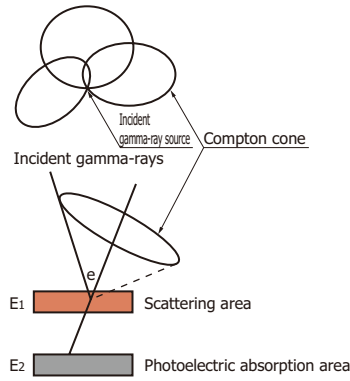


5 - 3 Si/CdTe Compton cameras

Compton cameras are detectors for measuring the energy and input direction of incident gamma-rays. These detectors are likely useful for applications such as observing gamma-rays arriving from space and visualizing the distribution of radioactive substances.

The Si/CdTe Compton camera detects the energy and input direction of incident gamma-rays from the energy (E_1) that the incident gamma-rays supplies to silicon electrons by Compton scattering, the energy (E_2) of the scattered gamma-rays, the position in the Si detector where Compton scattering takes place, and the position in CdTe where the scattered gamma-rays are photoelectrically absorbed. Hamamatsu double-sided SSDs are used as the Si detectors in Si/CdTe Compton cameras.^{18) 21) 22) 23) 24)}

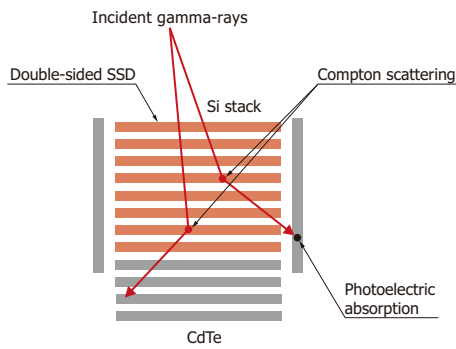
[Figure 5-6] Compton camera



(Courtesy of JAXA)

KSPDC0086EA

[Figure 5-7] Principle of Si/CdTe Compton camera



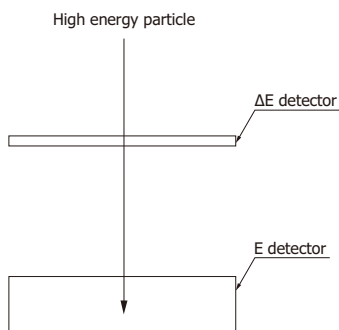
(Courtesy of JAXA)

KSPDC0087EA

5 - 4 ΔE -E detectors

ΔE -E detectors are used to identify particles. As shown in Figure 5-8, a transmission type ΔE detector is placed over a thick E detector. The ΔE detector detects the specific energy loss (dE/dx), and the total energy (E) of the particle is then calculated from the sum of the ΔE detector and E detector outputs. Here, the particle can be identified since the $(dE/dx) \times E$ value is unique to the type of particle. The incident angle and the position of the particle can be detected by using two PSDs as the ΔE detectors [Figure 5-9].^{7) 8)}

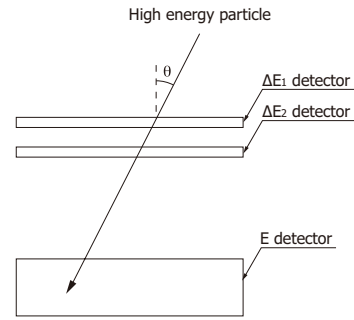
[Figure 5-8] ΔE -E detector



This is used when the incident angle is known.

KSPDC0073EA

[Figure 5-9] ΔE_1 - ΔE_2 -E detector



This is used when detecting the incident angle and position.

KSPDC0074EA

References

- 1) J. B. A. ENGLAND, et al., "CAPACITATIVE CHARGE DIVISION READ-OUT WITH A SILICON STRIP DETECTOR", Nucl. Instr. Meth. 185(1981)43-47
- 2) Tadayoshi DOKE, et al., "A NEW TWO DIMENSIONAL POSITION SENSITIVE DETECTOR WITH A GOOD LINEAR RESPONSE", Nucl. Instr. Meth. A261(1987)605-609
- 3) L. Evensen, et al., "RECENT DEVELOPMENT OF DETECTORS WITH INTEGRATED CAPACITORS AND POLYSILICON RESISTORS", IEEE Transactions on Nuclear Science, Vol.35, No.1, Feb. 1988, 428-431
- 4) Alan LITKE, et al., "A SILICON STRIP VERTEX DETECTOR FOR THE MARK II EXPERIMENT AT THE SLAC LINEAR COLLIDER", Nucl. Instr. Meth. A265(1988)93-98
- 5) P. Holl, et al., "A Double-Sided Si Strip Detector with Capacitive Readout and a New Method of Integrated Bias Coupling", IEEE Transactions on Nuclear Science, Vol.36, No.1, Feb. 1989, 251-255
- 6) T. YANAGIMACHI, et al., "NEW TWO-DIMENSIONAL POSITION SENSITIVE SILICON DETECTOR WITH GOOD POSITION LINEARITY AND RESOLUTION", Nucl. Instr. Meth. A275(1989)307-314
- 7) T. MOTOBAYASHI, et al., "PARTICLE IDENTIFICATION OF HEAVY IONS WITH LARGE SILICON DETECTORS", Nucl. Instr. Meth. A284(1989)526-528
- 8) N. Hasebe, et al., "Improvement of mass resolution of cosmic ray nuclei using a $\Delta E \times E$ Si detector telescope" Nucl. Instr. Meth. A325(1993)335-342
- 9) E. Barberis, et al., "Capacitances in silicon microstrip detectors", Nucl. Instr. Meth. A342(1994)90-95
- 10) V. Chabaud, et al., "The DELPHI silicon strip microvertex detector with double sided readout", Nucl. Instr. Meth. A368(1996)314-332
- 11) K. Hara, et al., "Prototype Si microstrip sensors for the CDF-II ISL detector", Nucl. Instr. Meth. A435(1999)437-445
- 12) T. Ohsugi, et al., "Design optimization of radiation-hard, double-sided, double-metal, AC-coupled silicon sensors", Nucl. Instr. Meth. A436(1999)272-280
- 13) C. Coldwey, "The ZEUS microvertex detector", Nucl. Instr. Meth. A447(2000)44-45
- 14) Y. Unno, "ATLAS silicon microstrip Semiconductor Tracker (SCT)", Nucl. Instr. Meth. A453(2000)109-120
- 15) T. Bergauer, et al., "Long-term stability test of Si strip sensors for the CMS tracker", Nucl. Instr. Meth. A494(2002)205-209
- 16) Stefan Schael, "The CMS silicon strip detector-mechanical structure and alignment system", Nucl. Instr. Meth. A511(2003)52-57
- 17) Luca Latronico, "The GLAST Large Area Telescope", Nucl. Instr. Meth. A511(2003)68-71
- 18) T. Takahashi, et al., "Hard X-ray and Gamma-Ray Detectors for the NEXT mission", New Astronomy Reviews, 48(2004)309-313
- 19) T. Ohsugi, et al., "Design and properties of the GLAST flight silicon microstrip sensors", Nucl. Instr. Meth. A541(2005)29-39
- 20) R. Stamen, et al., "Status of the Belle Silicon Vertex Detector", Nucl. Instr. Meth. A541(2005)61-66
- 21) Tadayuki Takahashi, et al., "Application of CdTe for the NeXT mission", Nucl. Instr. Meth. A541(2005)332-341
- 22) Shin Watanabe, et al., "A Si/CdTe Semiconductor Compton Camera", IEEE Transactions on Nuclear Science, 52-5(2005)2045-2051
- 23) S. Takeda, et al., "Development of Double-Sided Silicon Strip Detectors (DSSD) for a Compton Telescope", Nucl. Instr. Meth. A579(2007)859-865
- 24) S. Takeda, et al., "Experimental results of the gamma-ray imaging capability with a Si/CdTe semiconductor Compton camera", IEEE Transactions on Nuclear Science, 56-3(2009)783-790

Information described in this material is current as of June 2021.

Product specifications are subject to change without prior notice due to improvements or other reasons. This document has been carefully prepared and the information contained is believed to be accurate. In rare cases, however, there may be inaccuracies such as text errors. Before using these products, always contact us for the delivery specification sheet to check the latest specifications.

The product warranty is valid for one year after delivery and is limited to product repair or replacement for defects discovered and reported to us within that one year period. However, even if within the warranty period we accept absolutely no liability for any loss caused by natural disasters or improper product use. Copying or reprinting the contents described in this material in whole or in part is prohibited without our prior permission.

HAMAMATSU

www.hamamatsu.com

HAMAMATSU PHOTONICS K.K., Solid State Division

1126-1 Ichino-cho, Higashi-ku, Hamamatsu City, 435-8558 Japan, Telephone: (81)53-434-3311, Fax: (81)53-434-5184

U.S.A.: Hamamatsu Corporation: 360 Foothill Road, Bridgewater, N.J. 08807, U.S.A., Telephone: (1)908-231-0960, Fax: (1)908-231-1218, E-mail: usa@hamamatsu.com

Germany: Hamamatsu Photonics Deutschland GmbH: Arzbergerstr. 10, D-82211 Herrsching am Ammersee, Germany, Telephone: (49)8152-375-0, Fax: (49)8152-265-8, E-mail: info@hamamatsu.de

France: Hamamatsu Photonics France S.A.R.L.: 19, Rue du Saule Trapu, Parc du Moulin de Massy, 91882 Massy Cedex, France, Telephone: (33)1 69 53 71 00, Fax: (33)1 69 53 71 10, E-mail: infos@hamamatsu.fr

United Kingdom: Hamamatsu Photonics UK Limited: 2 Howard Court, 10 Tewin Road, Welwyn Garden City, Hertfordshire AL7 1BW, UK, Telephone: (44)1707-294888, Fax: (44)1707-325777, E-mail: info@hamamatsu.co.uk

North Europe: Hamamatsu Photonics Norden AB: Torshamnsgatan 35 16440 Kista, Sweden, Telephone: (46)8-509 031 00, Fax: (46)8-509 031 01, E-mail: info@hamamatsu.se

Italy: Hamamatsu Photonics Italia S.r.l.: Strada della Moia, 1 int. 6, 20044 Arese (Milano), Italy, Telephone: (39)02-93 58 17 33, Fax: (39)02-93 58 17 41, E-mail: info@hamamatsu.it

China: Hamamatsu Photonics (China) Co., Ltd.: 1201 Tower B, Jiaming Center, 27 Dongsanhuan Bellu, Chaoyang District, 100020 Beijing, P.R.China, Telephone: (86)10-6586-6006, Fax: (86)10-6586-2866, E-mail: hpc@hamamatsu.com.cn

Taiwan: Hamamatsu Photonics Taiwan Co., Ltd.: 8F-3, No. 158, Section2, Gongdao 5th Road, East District, Hsinchu, 300, Taiwan R.O.C. Telephone: (886)3-659-0080, Fax: (886)3-659-0081, E-mail: info@hamamatsu.com.tw

Cat. No. KSPD9002E02 Jun. 2021 DN